Running title: Oligomeric states of PSI, PSII, and LHCs in *ch1-1*

Corresponding Author:
Atsushi Takabayashi

Mailing address:
Institute of Low Temperature Science, Hokkaido University, N19 W8 Kita-Ku, Sapporo 060-0819, Japan
Phone: 86- 11-706-5493
Fax: 86- 11-706-5493
E-mail:takabayashi@pop.lowtem.hokudai.ac.jp

Subject areas:
(5) photosynthesis, respiration and bioenergetics
(4) proteins, enzymes and metabolism

Number of black and white figures, color figures and tables:
Number of black and white figures: 2
Number of color figures: 4
Number of tables: 4

Title: The Oligomeric States of the Photosystems and the Light-harvesting Complexes in the Chlorophyll *b*-less Mutant.

Authors:

Atsushi Takabayashi, Katsunori Kurihara, Masayoshi Kuwano, Yasuhiro Kasahara, Ryouichi Tanaka, Ayumi Tanaka.

Author's Addresses:

Institute of Low Temperature Science, Hokkaido University, N19 W8 Kita-Ku, Sapporo 060-0819, Japan

Abstract

The reversible associations between the light-harvesting complexes (LHCs) and the core complexes of PSI and PSII are essential for the photoacclimation mechanisms in higher plants. Two types of chlorophylls, chlorophyll *a* and chlorophyll *b*, both function in light harvesting and are required for the biogenesis of the photosystems. Chlorophyll *b*-less plants have been studied to determine the function of the LHCs because the chlorophyll *b* deficiency has severe effects specific to the LHCs. Previous studies have shown that the amounts of the LHCs, especially the LHCII trimer, were decreased in the mutants; however, it is still unclear whether chlorophyll *b* is required for the assembly of the LHCs and for the association of the LHCs with PSI and PSII. Here, to reveal the function of chlorophyll *b* in the LHCs, we investigated the oligomeric states of the LHCs, PSI, and PSII in the Arabidopsis chlorophyll *b*-less mutant. A two-dimensional blue native-PAGE/SDS-PAGE demonstrated that the PSI-LHCI supercomplex was fully assembled in the absence of chlorophyll *b*, whereas the trimeric LHCII and PSII-LHCII supercomplexes were not detected. The PSI-NAD(P)H dehydrogenase (NDH) supercomplexes were also assembled in the mutant. Furthermore, we detected two forms of monomeric LHC proteins. The faster migrating forms, which were detected primarily in the mutant, were likely apo-LHC proteins, whereas the slower migrating forms were likely the LHC proteins that contained chlorophyll *a*. These findings increase our understanding of the chlorophyll *b* function in the assembly of LHCs and the association of the LHCs with PSI, PSII,

and NDH.

Key words: chlorophyll *b*-less plant, photosystem, blue-native PAGE, *Arabidopsis thaliana*

Introduction

The protein and the pigment compositions of the peripheral light-harvesting complexes (LHCs) are highly variable among the oxygenic photosynthetic organisms (Schmid 2008), whereas those of the photosynthetic core complexes are well conserved. The LHCs in the green plant lineage, which includes the green algae and land plants, utilize chlorophyll *b* in addition to chlorophyll *a*, although the core complexes of both of the photosystems utilize only chlorophyll *a*. In these organisms, chlorophyll *b* is synthesized from chlorophyll *a* by chlorophyllide *a* oxygenase (CAO), which is conserved among the green algae and land plants (Tanaka et al. 1998, Tomitani et al. 1999).

The model plant *Arabidopsis thaliana* contains six Lhcb proteins (Lhcb1-6) and four Lhca proteins (Lhca1-4); these proteins function as the peripheral light-harvesting complexes of PSII and PSI, respectively (Schmid 2008). In addition, Lhca5 and Lhca6, which are two minor light-harvesting complex I proteins, are specifically involved in the formation of the PSI-NAD(P)H dehydrogenase (NDH) supercomplexes (Peng et al. 2009) and they have not yet been shown to function in light harvesting. The LHCs of PSII (LHCII) include the major LHCII proteins (Lhcb1-3) and the minor LHCII proteins (Lhcb4-6). The majority of the three major LHCII proteins are present in a heterotrimeric form (trimeric LHCII), whereas the minor LHCII proteins are present in a monomeric form (Schmid 2008). Moreover, the trimeric LHCII proteins can be associated with the dimeric PSII core complexes via the three minor Lhcb

proteins, which act as linkers (Caffarri et al. 2009). Such complexes are termed PSII-LHCII supercomplexes. In contrast, the peripheral light-harvesting complexes of PSI (LHCI) include the four Lhca proteins (Lhca1-4). The monomeric PSI core complex can be associated with the heterodimer of Lhca proteins (Lhca1-Lhca4 or Lhca2-Lhca3), and these complexes are termed the PSI-LHCI supercomplex (Jensen et al. 2007). In *Chlamydomonas reinhardtii*, the LHCI complex is predicted to be associated with the intermediate assembly complex of PSI, which is followed by the assembly of PsaG and PsaK (Ozawa et al. 2010). However, the functions of the chlorophyll molecules during the assembly of LHCI and the PSI-LHCI supercomplex remain unclear.

The reversible association between the multimeric LHCs and the PS core complexes is the main cause of the organizational changes in the PSI and PSII-LHCII supercomplexes. It is important to understand these changes because they are associated with major photoacclimation mechanisms (Eberhard et al. 2008). Specifically, the chlorophyll antenna size regulation and qE-quenching are regulated by the organizational changes that are primarily caused by the reversible association of LHCII with PSII (Tanaka and Melis 1997, Ballottari et al. 2007, Horton et al. 2008, de Bianchi et al. 2010). In contrast, the cyclic electron flow around PSI (CEF) that is mediated by NDH is regulated by the organizational changes that are caused by the interactions between the PSI-LHCI supercomplex and the specific LHCI proteins Lhca5 and

Lhca6 (Peng et al. 2009). The state transition for balancing the distribution of the light energy between the two photosystems is regulated by the organizational changes that are caused by the reversible association of the mobile LHCII with the PSI-LHCI supercomplex or the PSII-LHCII supercomplexes (Kargul and Barber 2008). Therefore, the oligomeric state changes that occur in the PSI-LHCI and PSII-LHCII supercomplexes are essential for photoacclimation in higher plants.

Chlorophyll *b*-less plants have been reported in Arabidopsis (Murray and Kohorn 1991, Espineda et al. 1999), barley (Highkin and Frenkel 1962), and rice (Terao et al. 1985). Although the LHCs contain both chlorophyll *a* and chlorophyll *b* molecules, the core complexes of PSI and PSII contain only chlorophyll *a*. Consequently, chlorophyll *b* deficiency causes severe effects on the LHCs without severely affecting the PSI and PSII core complexes. Therefore, chlorophyll *b*-less plants are useful tools for studying the functions and regulations of the LHCs.

Previous studies have reported the following phenotypes in Arabidopsis chlorophyll *b*-less plants: pale-green leaves, retarded growth, decreased photosynthetic performance, and an increased susceptibility to high light (Murray and Kohorn 1991, Tanaka and Tanaka 2005, Havaux et al. 2007, Kim et al. 2009). The decrease in the levels of the LHC proteins is at least partially responsible for the chlorophyll *b*-less mutant phenotypes. The mRNAs of LHC proteins were shown to be normally expressed and translated into the LHC apoproteins (Preiss

and Thornber 1995). Next, the LHC apoproteins are integrated into the thylakoid membranes and are likely assembled with only chlorophyll *a* (Preiss and Thornber 1995). However, the accumulation of LHC proteins, especially those of the major LHCII proteins, was significantly decreased (Tanaka and Tanaka 2005, Havaux et al. 2007, Kim et al. 2009). In addition, the decreased levels of the LHC proteins were highly varied depending on each protein and on the growth conditions (Tanaka and Tanaka 2005). These data suggest that chlorophyll *b* is required for the assembly or the stabilization of the LHCs.

In addition, the organizational changes in the PSI and PSII supercomplexes likely contribute to the phenotypes of the chlorophyll *b*-less plants. Several studies utilized native PAGE techniques, which included the "green-gel" analysis and Deriphat-PAGE, to examine these changes (Murray and Kohorn 1991, Preiss and Thornber 1995, Havaux et al. 2007). According to the previous reports, the trimeric LHCII, PSII-LHCII supercomplexes, and PSI-LHCI supercomplex were not detected in the chlorophyll *b*-less mutants, although the oligomeric states of those supercomplexes still remain unclear. The major reason of the poor understanding of their oligomeric states is that the conventional native PAGE techniques did not separate the high-molecular-weight supercomplexes with high resolution. In addition, when native PAGE techniques are used, it is difficult to keep labile protein complexes intact during the electrophoresis. Because the PSII-LHCII supercomplexes are especially large and labile

(Caffarri et al. 2009), electrophoresis methods that are more appropriate for such complexes are required.

BN-PAGE was recently developed to separate structurally and enzymatically intact protein complexes at high resolution (reviewed by Wittig and Schägger 2009). Because BN-PAGE typically has a better resolution capacity for large and labile protein complexes when compared to conventional techniques, a BN-PAGE analysis can yield more detailed information regarding the oligomeric states of the supercomplexes of PSI and PSII in the chlorophyll *b*-less mutant. Kim et al. (2009) recently utilized BN-PAGE to separate the pigment-protein complexes in the Arabidopsis chlorophyll *b*-less mutant, and the authors reported the presence of the PSII core complexes (in their monomeric and dimeric forms) and the putative PSI core complex, which contained a reduced antenna size. However, because their identification was based on the electrophoretic mobilities of the protein complexes that were detected by CBB staining, the validity of their identification and the precise subunit compositions of those complexes remained unclear. In addition, the minor protein complexes were not likely detected because of the relatively poor sensitivity of the CBB staining technique.

To reveal the function of chlorophyll *b* in the assembly of the LHCs, the PSI-LHCI supercomplex, and the PSII-LHCII supercomplexes, we report here detailed information regarding the oligomeric states of these pigment-protein complexes in the Arabidopsis

chlorophyll *b*-less mutant; our analyses were primarily based 2D-BN/SDS-PAGE, which was followed by CBB staining and an immunoblot analysis.

Results

Phenotypes of *ch1-1*.

The *ch1* mutant was the first characterized Arabidopsis mutant that displayed the chlorophyll *b*-less phenotype (Murray and Kohorn 1991). This phenotype is caused by impairment of the *CAO* gene, which is a gene that is essential for chlorophyll *b* biosynthesis (Espineda et al. 1999). Previous studies have reported that *ch1-1* plants, which carry a null allele of *ch1*, completely lack chlorophyll *b* (Oster et al. 2000, Tanaka and Tanaka 2005). In fact, chlorophyll *b* was not present in *ch1-1*, and its chlorophyll *a* content was slightly reduced to 74% of that in the wild type (Table 1). In addition, the *ch1-1* mutant displayed the visible phenotypes of pale-green leaves and delayed growth (Fig. 1). Furthermore, chlorophyll fluorescence measurements showed that the NPQ (non-photochemical quenching) was decreased by approximately 30% in *ch1-1*, whereas the Fv/Fm (the maximal quantum yield of PSII) was slightly decreased (Table 2). Among the three components (qE, qT, qI) of the NPQ, the decrease in qE was the primary cause of the decreased NPQ that was observed in *ch1-1* (Table 2). The qE in the mutant was approximately 60% of the level in the wild type despite the complete loss of chlorophyll *b*.

These phenotypes were consistent with previous reports of the Arabidopsis chlorophyll *b*-less mutants (Tanaka and Tanaka 2005, Havaux et al. 2007, Kim et al. 2009).

Proteomic comparison of the thylakoid membranes.

To compare the accumulated levels of the LHCs that were normalized to the level of chlorophyll *a* between the wild type and *ch1-1*, an immunoblot analysis was performed. The Lhcb1 and Lhcb6 protein levels were substantially decreased in *ch1-1*, whereas the level of Lhcb5 was slightly increased. The levels of the Lhcb2, Lhcb3, Lhcb4, and Lhca proteins were slightly decreased or were not markedly changed (Fig. 2).

Furthermore, to detect the changes in the protein compositions of PSI and PSII between wild-type and *ch1-1* plants, we applied a proteomic analysis of the thylakoid membranes, which utilized nanoscale liquid chromatography combined with electrospray ionization tandem mass spectrometry (ESI-LC-MS/MS).

A total of 618 proteins in the wild type and 466 proteins in *ch1-1* were identified in the purified thylakoid membranes (Supplemental Tables 1 and 2). Of those proteins, 325 were detected in both the wile type and *ch1-1*. The 13 subunits of the PSI core complex and the Lhca1-6 proteins were identified for the PSI proteins in both wild-type and the *ch1-1* plants (Table 3). The 17 subunits of the PSII core complex and the Lhcb1-6 proteins were also

identified for the PSII proteins in both wild-type and *ch1-1* plants (Table 3). These data suggest that the PSI and PSII protein compositions did not markedly change in *ch1-1*. Notably, some of the PSI and PSII proteins were not identified in either of the genotypes in this study; this may have resulted because the likelihood of the MS-based protein detection varied greatly depending on the properties of each peptide, such as the peptide length, net charge, and solubility (Lu et al. 2007). Specifically, the probability of identifying a small protein was low because the number of the unique peptides in small proteins is less than that in large proteins.

The oligomeric states of the pigment-protein complexes were substantially changed in the *ch1-1* plants.

Next, we further investigated the oligomeric forms of these supercomplexes in *ch1-1*. The purified thylakoid membranes were solubilized with dodecyl maltoside and were then separated by BN-PAGE with 4-14% linear gradient gels.

The differences in the separation patterns of the pigment-protein complexes by BN-PAGE between wild-type and *ch1-1* plants are shown in Fig. 3. The PSII-LHCII supercomplexes, the PSI-LHC supercomplex, the LHCII assembly (CP29-CP24-trimeric LHCII supercomplex), and the trimeric LHCII were not detected in *ch1-1* (Fig. 3), which is consistent with the results of previous reports (Havaux et al. 2007, Kim et al. 2009). In contrast, the

dimeric PSII, the monomeric PSI, and the monomeric PSII markedly accumulated in *ch1-1* (Fig. 3). Notably, the green band that corresponded to the monomeric LHC proteins was observed both in wild-type and *ch1-1* plants.

The subunit compositions of the PSI and PSII core complexes did not markedly change in *ch1-1* plants.

To confirm the identification of the protein complexes that are shown in Fig. 3, and to compare the subunit compositions of these protein complexes, we performed second-dimension SDS-PAGE that was followed by CBB staining (Fig. 4A and 4B). The CP43-less PSII was identified in both wild-type and *ch1-1* plants in addition to the pigment-protein complexes that were identified in Fig. 3. In addition, the subunits of the ATP synthase and cytochrome b_6/f complexes were identified in both wild-type and *ch1-1* plants (Fig. 4A and 4B). We observed no differences in the subunit compositions of the commonly identified pigment-protein complexes (dimeric PSII, monomeric PSII, CP43-less PSII, and monomeric PSI) in both wild-type and *ch1-1* plants (Fig. 4A and 4B), which correlated with the predictions of the proteomic analysis (Table 3). In addition, the PSII-LHCII supercomplexes, PSI-LHCI supercomplex, LHCII assembly, and trimeric LHCII were not detected in *ch1-1* by CBB-staining, which is consistent with the results of previous studies (Havaux et al. 2007, Kim et al. 2009).

The PSI-LHCI supercomplex was assembled without chlorophyll *b*.

The immunoblot analysis typically demonstrates a higher sensitivity and specificity for the detection of proteins than that of CBB staining. Therefore, to further investigate the oligomeric states of the PSI and PSII supercomplexes with a high sensitivity, we performed an immunoblot analysis.

The LHCII trimer and the PSII-LHCII supercomplexes were not detectable in the *ch1-1* plants by the immunoblot analyses of the PSII core proteins (CP43, CP47) and the Lhcb proteins (Lhcb1-6) (Fig. 5B). In contrast, the PSI-LHCI supercomplex was detected in *ch1-1* by the immunoblot analyses of the PSI core proteins (PsaA/PsbB) and the Lhca proteins (Lhca1-4), although the accumulation ratio of the PSI-LHCI supercomplex to the monomeric PSI was much lower than in the wild type (Fig. 5A and 5B). To our knowledge, this is the first indication that the PSI-LHCI supercomplex is present in chlorophyll *b*-less plants. The presence of the PSI-LHCI supercomplex demonstrated that the LHCI dimer and the PSI-LHCI supercomplex were able to be assembled in the absence of chlorophyll *b*.

The PSI-NDH supercomplex was also assembled without chlorophyll *b*.

Recent data regarding the subunit composition and the structure of the NDH complex have

shown that the NDH complex interacts with the PSI-LHCI supercomplex and forms the PSI-NDH supercomplex (Peng et al. 2010). The PSI-NDH supercomplex was shown to be essential for the efficient operation of the NDH-dependent cyclic electron flow, although neither the stoichiometry nor the structure was determined (Peng et al. 2009). In this study, we detected two or three bands that contained the PSI-NDH supercomplexes by performing an immunoblot analysis of NDF1, which is a subunit of the NDH complex, and of PsaA/PsaB (Fig. 5A and 5B). This report is the first to describe the presence of the PSI-NDH supercomplexes in the chlorophyll *b*-less plants. The presence of the PSI-NDH supercomplex implied that the cyclic electron flow around PSI via NDH worked in *ch1-1*.

The monomeric LHCI and LHCII proteins were assembled with chlorophyll a in ch1-1.

Two forms of the monomeric LHC proteins were detected by CBB staining and the immunoblot analysis (Fig. 4B and 5B). The faster-migrating forms of the monomeric LHC proteins (Lhca1-4 and Lhcb1-6) accumulated to a significant level in *ch1-1* (Fig. 5B), whereas the faster-migrating forms of the monomeric proteins Lhca2 and Lhcb3 only slightly accumulated in wild-type plants (Fig. 5A). The slower-migrating forms were the most predominant forms of the monomeric LHCs in wild-type plants (Fig. 5A). Therefore, we hypothesized that the slower-migrating forms were the normal monomeric LHCs and the faster-migrating forms of the

monomeric Lhcb proteins were the apoproteins that lacked chlorophylls.

To determine whether the faster-migrating forms of the monomeric LHC proteins were the apo-LHC proteins that lacked chlorophyll, we extracted the native forms of the trimeric LHCII proteins from the 1D-BN-gel and investigated the effect of heat treatment on the LHCII. The electrophoretic mobility of the extracted trimeric LHCII was identical to that of the untreated trimeric LHCII, which suggests that the extracted trimeric LHCII retained its native form. Following the heat treatment, the following three bands of Lhcb2 were detected: the trimeric LHCII, the monomeric LHCII and the fastest-migration band (Fig. 6). Because the fastest-migration band emerged following the heat treatment, it was likely the apo-Lhcb2 protein. In addition, a previous report showed that heat treatment can cause the release of chlorophyll from chlorophyll-binding proteins, and apoproteins that are not associated with chlorophyll show a faster migration than their native forms (Tanaka 1987). These data suggested that the monomeric LHC proteins that contained chlorophyll *a* were assembled and accumulated in *ch1-1*.

Discussion

In this study, we examined the impact of chlorophyll *b* deficiency on the PSI and PSII-LHCII supercomplexes by using BN-PAGE. First, we detected a small amount of the PSI-LHCI supercomplex in *ch1-1*. The PSI-LHCI supercomplex was fully assembled in *ch1-1* because the

supercomplex displayed the same electrophoretic mobility as the PSI-LHCI supercomplex that was isolated from wild-type plants (Fig. 5) and because we did not observe any differences in the subunit composition of PSI by proteomic analysis (Table 3). The presence of the PSI-LHCI supercomplex in *ch1-1* implies that the dimeric LHCIs are assembled, and chlorophyll *b* is not required for the assembly of the PSI-LHCI supercomplex. Notably, red algae possess LHCs that can bind to chlorophyll *a* and associate strictly with PSI (Tan et al. 1997a, Tan et al. 1997b, Busch and Hippler 2010). The dimeric LHCIs and the PSI-LHCI supercomplex are expected to be unstable in *ch1-1* because the levels of these protein complexes were decreased to a level that was undetectable by CBB staining (Fig. 4B). One explanation for the low accumulation of the PSI-LHCI supercomplex in *ch1-1* is that the PSI-LHCI supercomplex tends to be degraded or dissociated into the monomeric PSI and the monomeric LHCI based on its instability; this should not be a problem for the assembly of the PSI-LHCI supercomplex. Alternatively, the assembly of the PSI-LHCI supercomplex from the monomeric PSI and LHCIs was potentially inefficient. Further studies will be necessary to lend further support to this hypothesis.

Similarly, the monomeric LHCI proteins were relatively more unstable in *ch1-1* than in the wild type because the level of putative apo-LHC proteins increased significantly (Fig. 5B). Kim et al. (2009) predicted that most PSI complexes that are present in *ch1-1*, which displayed an electrophoretic mobility that was higher than that of the typical PSI-LHCI supercomplex, would

be PSI-LHCI supercomplexes with a reduced antenna size. However, our immunoblot analysis of the Lhca proteins showed that the fast-migrating PSI complex was likely to be the monomeric form of the PSI complex that lacked the LHCI (Fig. 4B). These data suggest that chlorophyll *b* is not necessary for the assembly of the PSI-LHCI supercomplex but that it is required for the stabilization of the multimeric LHCIs and the PSI-LHCI supercomplex.

Based on the immunoblot analysis, in addition to the PSI-LHCI supercomplex, the PSI-NDH supercomplexes were also assembled in *ch1-1* (Fig. 5B). This finding was also supported by the proteomic data, which suggested that all the four of the NDH subcomplexes (the membrane subcomplex, subcomplexes A and B, and the lumen subcomplex) (Peng et al. 2010) were expected to be present in *ch1-1* because at least one protein from each subcomplex was identified (Table 4). Furthermore, many of the NDH proteins were shown to be required for the accumulation of the NDH complex (Peng et al. 2010), which suggests that the intact NDH complex was likely formed in *ch1-1*. The Lhca5 and Lhca6 proteins are required for the formation of the PSI-NDH supercomplexes (Peng et al. 2009, Peng and Shikanai 2011). The PSI-NDH supercomplexes did not accumulate in the *lhca5/lhca6* double mutant; however, the monomeric NDH complex was detected in the double mutant (Peng and Shikanai 2011). In addition, the smaller NDH-PSI supercomplexes have been detected in the *lhca6* single mutant, whereas the full-size and the smaller NDH-PSI supercomplexes have been detected in the *lhca5*

single mutant (Peng and Shikanai 2011). Therefore, the presence of the PSI-NDH supercomplexes in *ch1-1* demonstrated that Lhca5 or/and Lhca6 could function as a linker to join the PSI and the NDH complexes even in *ch1-1*. Notably, the Lhca5 and Lhca6 proteins were identified in *ch1-1* by the proteomic approach (Table 3). However, the association of the Lhca1-4 proteins with the PSI-NDH supercomplexes was not observed in the immunoblot analysis. Therefore, it is unclear whether the PSI-LHCI or the PSI monomer interacted with the NDH complex. It is likely that both of these options are possible.

We detected two forms of the monomeric LHC proteins in *ch1-1* (Fig. 4B and 5B). We further showed that the slower-migrating forms were expected to be monomeric LHCs that contained chlorophyll *a* and that the faster-migrating forms of the LHC proteins were likely to constitute the apo-LHC proteins that lacked chlorophyll *a*. Notably, some of the major LHCIIs likely aggregated following the heat treatment and did not pass through the stacking gel, even in the presence of dodecyl maltoside.

The presence of the monomeric LHCI proteins that contained chlorophyll *a* in the Arabidopsis chlorophyll *b*-less mutants has been reported previously based on the absorption and CD spectra (Havaux et al. 2007). Meanwhile, Schmid et al. (2002) reported that the *in vitro* reconstitution of the Lhca proteins in the absence of chlorophyll *b* resulted in the formation of the LHC in the recombinant Lhca1 (rLhca1) and rLhca3; however, the rLhca2 and rLhca4

proteins were not formed in the absence of chlorophyll *b*. This result appears to be contradictory to our data because we detected the putative monomeric Lhca2 and Lhca4 proteins that contained chlorophyll *a* (Fig. 5B). However, according to previous reports (Schmid et al. 2002, Wientjes and Croce 2011), it was not possible to reconstitute the Lhca2/3 dimer *in vitro* even in the presence of both chlorophyll *a* and chlorophyll *b*, although the reconstituted Lhca1/4 dimer was formed in the same condition. Therefore, mechanisms that assist with the assembly of LHCI *in vivo* may exist, and this could explain the presence of the four monomeric Lhca1-4 proteins that contained chlorophyll *a* and the dimeric LHCIs in *ch1-1*.

In contrast to the PSI-LHCI supercomplex, the trimeric LHCII, the LHCII assembly, and the PSII-LHCII supercomplexes were not detected (Fig. 4B and 5B), which confirmed the findings of previous studies (Havaux et al. 2007, Kim et al. 2009). Kim et al. (2009) reported that the monomeric PSII was the predominant form of the PSII core complex in *ch1-3*, which is another allele of *ch1*; however, we observed substantial levels of the dimeric PSII that were comparable to the amounts of the monomeric PSII in *ch1-1* (Fig. 3). One possible explanation of this inconsistency is that the dimeric PSII in *ch1-1* may be easily dissociated during the solubilization and electrophoresis processes as suggested by Kim et al. (2009). Meanwhile, we found that the monomeric LHCII proteins that contained chlorophyll *a* accumulated in the *ch1-1* plants (Fig 4B, 5B, and 6)*;* this result was not reported in previous studies (Espineda et al. 1999,

Havaux et al. 2007). The presence of the monomeric LHCII proteins that contained chlorophyll *a* suggested that chlorophyll *b* was not necessarily required for the assembly of the monomeric LHCII but that it was required for the trimerization of the LHCII.

The oligomeric state changes of PSI, PSII, and the LHCs may be responsible for the phenotypes of *ch1-1*. The Arabidopsis chlorophyll *b*-less mutants are highly susceptible to high levels of light, although the PSII antenna size in the mutants is much smaller than in the wild type (Havaux et al. 2007; Kim et al. 2009). According to the chlorophyll fluorescence measurements, the qE decreased but was not eliminated in *ch1-1* (Table 2), which is consistent with the results of previous reports (Havaux et al. 2007, Kim et al. 2009). Because the trimeric LHCII and PSII-LHCII supercomplexes were not detected, most of the qE in *ch1-1* is expected not depend on the trimeric LHC II or PSII-LHCII supercomplexes, but it is likely responsible for the reaction center quenching in the PSII core complexes as suggested by the previous paper (Havaux et al. 2007). Notably, the *ch1* mutants were reported to release a higher level of singlet oxygen in high light than the wild type (Dall'Osto et al. 2010). In addition, the suppression of zeaxanthin in the *ch1* background resulted in the accumulation of severe photo-oxidative damage in high light; this result demonstrates that zeaxanthin plays an important role in the protection of the thylakoid membranes from photo-oxidative damage even in the LHCII-defective *ch1* mutant (Havaux et al. 2007, Dall'Osto et al. 2010). These data suggest that

the reaction center of PSII in the chlorophyll *b*-less mutants causes a higher level of singlet oxygen in high light because of the absence of the LHCII-dependent protective mechanisms, which include thermal dissipation.

In addition, the stacking of the grana in *ch1-3* was reported to be decreased, although it was still substantially present, and the accumulation of Lhcb5 in the mutant was shown to contribute to the formation of the grana stacking (Kim et al. 2009). Because Lhcb5 accumulated in the monomeric form (Fig. 4B), the monomeric form of Lhcb5 is expected to contribute to the formation of the grana stacking in the Arabidopsis chlorophyll *b*-less mutants. Similar to monomeric Lhcb5, other monomeric LHC proteins may participate in the formation of the grana stacking in *ch1-1*. Furthermore, we demonstrated the presence of the PSI-NDH supercomplex in *ch1-1*. Previous studies have revealed that the NDH-defective mutants were susceptible to oxidative stresses under various environmental conditions, such as high light, drought, and high or low temperatures (Endo et al. 1999, Horváth et al. 2000, Li et al. 2004, Wang et al. 2006). The contribution of the cyclic electron flow around PSI to the phenotype of the chlorophyll *b*-less plants was unclear; however, the presence of the PSI-NDH supercomplex suggested that the NDH-dependent cyclic electron flow around PSI may play a role in preventing photoinhibition in *ch1-1*.

We hypothesize that the LHCI proteins can bind to chlorophyll *a* without

simultaneously binding to chlorophyll *b* because the LHCI proteins are likely to be assembled with chlorophyll *a*. According to the i*n vitro* reconstitution analyses, the chlorophyll binding sites in the LHCI and LHCII showed the different affinities for chlorophyll *a* and chlorophyll *b*. However, considerable flexibility was shown in their specificity for chlorophyll *a* or chlorophyll *b* (Reviewed by Schmid 2008). For example, the chlorophyll *b*-binding sites of Lhca4, which were reconstituted in the absence of chlorophyll *b*, were reported to be occupied by chlorophyll *a* (Schmid et al. 2002). Therefore, the chlorophyll *b* binding sites in the LHCI proteins were likely occupied with chlorophyll *a*. It is clear that the dimeric LHCIs (Lhca1-Lhca4 and Lhca2-Lhca3) and even the PSI-LHCI supercomplex can be assembled in the absence of chlorophyll *b* because the PSI-LHCI supercomplex accumulated in the *ch1-1* plants. However, the decrease in the amounts of the PSI-LHCI supercomplex and the dimeric LHCIs suggests that the incorporation of chlorophyll *b* into the LHCI may be important for the stabilization of the multimeric LHCI. Because the mechanism of the assembly of the LHCs with the chlorophyll molecules remains unclear, we propose that the chlorophyll *b*-less plants will be helpful in future studies. Further studies will reveal not only the functions of the LHCs but the assembly of the LHCs and the supercomplexes of PSI and PSII.

Materials and Methods

Plant material and growth conditions

The Columbia ecotype of *Arabidopsis thaliana* was used as the wild type, and *ch1-1*, which displays a completely impaired chlorophyll *b* biosynthesis (Oster et al. 2000), was used as the chlorophyll *b*-less mutant in this study. All of the plants were grown in soil under constant illumination (70 μmol photons m^{-2} s^{-1}) at 23°C.

Chlorophyll determination

The chlorophyll content of 4-week-old wild-type and *ch1-1* plants was determined according to Porra et al. (1989).

Chlorophyll fluorescence measurements

Chlorophyll fluorescence was measured with a PAM-2000 portable fluorometer (Walz, Effeltrich, Germany). The maximum chlorophyll fluorescence (Fm) was measured after the plants had been dark-adapted for 20 min. Following the illumination with an actinic light for 10 min (500 μmol photons m^{-2} s^{-1}), the qE component of the NPQ was calculated as (Fm/Fm')-(Fm/Fm"), where the maximum yield of the chlorophyll fluorescence during the illumination was Fm', and after the dark relaxation for 10 min, it was Fm".

Total leaf protein extraction

The total leaf proteins were extracted from the leaves of 4-week-old plants (wild type) and 5-week-old plants (*ch1-1*). At these growth stages, both the wild type and the *ch1-1* mutant contained approximately the same number of leaves (12-13 leaves). Total protein was extracted from the leaf material using SDS sample buffer (63 mM Tris-HCl (pH 6.8), 10% glycerol, and 2% SDS). After centrifugation at 18,800 *g* for 10 min at 25°C, the supernatants (which corresponded to 2 μg of chlorophyll *a*) were loaded onto an SDS-PAGE gel (14% acrylamide gel) and were transferred to PVDF membranes for the immunoblot analysis.

Isolation and fractionation of the chloroplasts

The intact chloroplasts were prepared from the leaves of 4-week-old plants (wild type) and 5-week-old plants (*ch1-1*). The leaves were homogenized in ice-cold isolation buffer that contained 20 mM Tricine-NaOH (pH 8.0), 0.45 M sorbitol, 10 mM EDTA-2Na, 1 mM $NaHCO_3$, 0.1% (w/v) BSA, 0.05% (w/v) DTT, and 0.05% (w/v) PVP. The homogenate was immediately filtered through 4 layers of Miracloth and then centrifuged at 1,000 *g* for 5 min at 4°C. The pellet was suspended in ice-cold wash buffer that contained 20 mM MOPS-NaOH (pH 7.6), 0.33 M sorbitol, 5 mM $MgCl_2$, and 2.5 mM EDTA-2Na. The suspension was loaded onto a 40%/80% Percoll step gradient in the same buffer. After centrifugation at 3,000 *g* for 10 min at 4°C, the intact chloroplasts at the interface of 40% and 80% were collected.

The intact chloroplast suspension was diluted 5-fold with ice-cold wash buffer and was centrifuged at 1,000 *g* for 5 min at 4°C. The pellet was osmotically ruptured in ice-cold swelling buffer that contained 10 mM MOPS-NaOH (pH 7.6) and 4 mM $MgCl_2$, and it was loaded onto a sucrose gradient (2 M, 0.93 M and 0.6 M). After centrifugation at 95,000 *g* in a RPS56T rotor (Hitachi, Tokyo, Japan) for 60 min at 4°C, the purified thylakoid membranes were collected from the interface between the 0.93 M layer and the 2 M layer.

1D SDS-PAGE and nano-LC/MS/MS for the thylakoid membrane proteomics

The purified thylakoid membranes (which corresponded to 20 μg of protein) were solubilized and separated by SDS-PAGE using commercial gels (15%, e-PAGEL; ATTO, Tokyo, Japan), according to the manufacturer's protocol. The SDS-gel strips were cut horizontally into approximately 70 pieces from the top to the bottom. All of the gel pieces were treated by in-gel trypsin digestion (Roche, Tokyo, Japan) according to Shevchenko et al. (1996). The LC-MS/MS analyses were performed using LTQ that was coupled with HPLC (ThermoFisher Scientific, Yokohama, Japan). The resulting peptides were loaded onto an L-column2 ODS column that was packed with C18 (5 μm, 12 nm pore size) (Chemicals Evaluation and Research Institute, Tokyo, Japan) and were separated by a gradient using solvent A (2% acetonitrile in 0.1% formic acid) and solvent B (90% acetonitrile in 0.1% formic acid). The gradient condition was 95% A

and 5% B to 10% A and 90% B. The separated peptides were applied to an LTQ for the MS/MS analysis. Protein identification was performed by searching the TAIR9 database (The Arabidopsis Information Resource) with the Mascot program version 2.2 (Matrix Science, Tokyo, Japan). The following search parameters were used: 0.05 threshold of the ion score cutoff; 1.2 Da peptide tolerance; ±0.8 Da MS/MS tolerance; 1+, 2+, or 3+ peptide charge; trypsin digestion with two missed cleavages allowed; carbamidomethyl modification of the cysteines as a fixed modification; and the oxidation of methionine as a variable modification.

2D-BN/SDS-PAGE

BN-PAGE was performed essentially according to the methods that were described by Wittig et al. (2006). The purified thylakoid membranes were prepared essentially according to the methods that were described by Salvi et al. (2008). Briefly, the purified thylakoid membrane proteins (which corresponded to 4 μg of chlorophyll) were suspended in ice-cold resuspension buffer that contained 50 mM imidazole-HCl (pH 7.0), 20% glycerol, 5 mM 6-aminocaproic acid, and 1 mM EDTA-2Na and were then solubilized with 1% (w/v) dodecyl maltoside on ice for 5 min at a detergent to chlorophyll ratio of 10:1. After centrifugation at 18,800 *g* for 10 min at 4°C, the supernatants were supplemented with Coomassie Blue solution [5% (w/v) Serva Blue G (Serva, Heidelberg, Germany), 500 mM 6-aminocaproic acid, and 50 mM Imidazole-HCl (pH

7.0)] at a detergent/Coomassie ratio of 4/1 (w/w) and separated on 4-13% polyacrylamide gradient gels.

For the second-dimension of SDS-PAGE, the BN gel strips were soaked for 1 h at room temperature in a solution that contained 1% (w/v) SDS and 1% (v/v) 2-mercaptoethanol and run on a second-dimension SDS-PAGE gel (14% polyacrylamide gels that contained 4 M urea). The proteins were separated on the second-dimension SDS-PAGE using the Laemmli buffer system (Laemmli 1970).

CBB-staining and immunoblot analysis

For the CBB staining and immunoblot analysis, the proteins were blotted onto PVDF membranes with transfer buffer (25 mM Tris, 192 mM glycine, 20% methanol) using a wet transfer method. The proteins were visualized using the Quick-CBB kit (Wako chemicals, Osaka, Japan) or detected using the Western Lightning Chemiluminescence Reagent Plus (Perkin Elmer Life Sciences, Yokohama, Tokyo). Antibodies that were directed against the CP43, CP47, Lhca1-4 and Lhcb1-6 proteins were purchased from Agrisera. The anti-PsaA/PsaB and anti-NDF1 antibodies were described previously (Tanaka et al. 1991, Takabayashi et al. 2009).

Heat denaturation of trimeric LHCII

The band of the trimeric LHCII that was separated with BN-PAGE was excised and homogenized in a buffer that contained 50 mM imidazole-HCl (pH 7.0), 20% glycerol, 5 mM 6-aminocaproic acid, 1 mM EDTA-2Na, and 1% dodecyl maltoside. After a 5-min incubation on ice, each sample was centrifuged at 18,800 *g* for 10 min at 4°C, and the supernatant was used as the trimeric LHCII solution. The trimeric LHCII was heated for 1 min at 90°C, with stirring at 20-second intervals to avoid aggregation, and it was separated with BN-PAGE. The oligomeric states of the LHCII were detected by an immunoblot analysis with the anti-Lhcb2 antibodies.

Funding

This work was supported by the Grants-in-Aids for Young Scientists (09153533 to A.T.) and by Scientific Research (17770027 to R.T.) from the Japan Society for the Promotion of Science.

Reference

Ballottari, M., Dall'Osto, L., Morosinotto, T. and Bassi, R. (2007) Contrasting behavior of higher plant photosystem I and II antenna systems during acclimation. *J. Biol. Chem.* 282: 8947-8958.

Busch, A. and Hippler, M. (2010) The structure and function of eukaryotic photosystem I. *Biochim. Biophys. Acta* 1807: 864-877.

Caffarri, S., Kouril, R., Kereiche, S., Boekema, E.J. and Croce, R. (2009) Functional

architecture of higher plant photosystem II supercomplexes. *EMBO J.* 28: 3052-3063.

Dall'Osto, L., Cazzaniga, S., Havaux, M. and Bassi, R. (2010) Enhanced photoprotection by protein-bound vs free xanthophyll pools: a comparative analysis of chlorophyll *b* and xanthophyll biosynthesis mutants. *Mol. Plant* 3: 576-593.

de Bianchi, S., Ballottari, M., Dall'osto, L. and Bassi, R. (2010) Regulation of plant light harvesting by thermal dissipation of excess energy. *Biochem. Soc. Trans.* 38: 651-660.

Eberhard, S., Finazzi, G. and Wollman, F.A. (2008) The dynamics of photosynthesis. *Annu. Rev. Genet.* 42: 463-515.

Endo, T., Shikanai, T., Takabayashi, A., Asada, K. and Sato, F. (1999) The role of chloroplastic NAD(P)H dehydrogenase in photoprotection. *FEBS Lett.* 457: 5-8.

Espineda, C.E., Linford, A.S., Devine, D. and Brusslan, J.A. (1999) The *AtCAO* gene, encoding chlorophyll *a* oxygenase, is required for chlorophyll *b* synthesis in *Arabidopsis thaliana*. *Proc. Natl Acad. Sci. USA* 96: 10507-10511.

Fu, A., He, Z., Cho, H.S., Lima, A., Buchanan, B.B. and Luan, S. (2007) A chloroplast cyclophilin functions in the assembly and maintenance of photosystem II in *Arabidopsis thaliana*. *Proc. Natl Acad. Sci. USA* 104: 15947-15952.

Havaux, M., Dall'osto, L. and Bassi, R. (2007) Zeaxanthin has enhanced antioxidant capacity with respect to all other xanthophylls in Arabidopsis leaves and functions independent of binding to PSII antennae. *Plant Physiol.* 145: 1506-1520.

Highkin, H.R. and Frenkel, A.W. (1962) Studies of growth & metabolism of a barley mutant lacking chlorophyll *b*. *Plant Physiol.* 37: 814-820.

Horton, P., Johnson, M.P., Perez-Bueno, M.L., Kiss, A.Z. and Ruban, A.V. (2008) Photosynthetic acclimation: does the dynamic structure and macro-organisation of photosystem II in higher plant grana membranes regulate light harvesting states? *FEBS J.* 275: 1069-1079.

Horváth, E.M., Peter, S.O., Joët, T., Rumeau, D., Cournac, L., Horváth, G.V. et al. (2000) Targeted inactivation of the plastid *ndhB* gene in tobacco results in an enhanced sensitivity of

photosynthesis to moderate stomatal closure. *Plant Physiol.* 123: 1337-1350.

Jensen, P.E., Bassi, R., Boekema, E.J., Dekker, J.P., Jansson, S., Leister, D.et al. (2007) Structure, function and regulation of plant photosystem I. *Biochim. Biophys. Acta* 1767: 335-352.

Kargul, J. and Barber, J. (2008) Photosynthetic acclimation: structural reorganisation of light harvesting antenna--role of redox-dependent phosphorylation of major and minor chlorophyll *a*/*b* binding proteins. *FEBS J.* 275: 1056-1068.

Kim, E.H., Li, X.P., Razeghifard, R., Anderson, J.M., Niyogi, K.K., Pogson, B.J. et al. (2009) The multiple roles of light-harvesting chlorophyll *a*/*b*-protein complexes define structure and optimize function of Arabidopsis chloroplasts: a study using two chlorophyll *b*-less mutants. *Biochim. Biophys. Acta* 1787: 973-984.

Laemmli, U.K. (1970) Cleavage of structural proteins during the assembly of the head of bacteriophage T4. *Nature* 227: 680-685.

Li, X.G., Duan, W., Meng, Q.W., Zou, Q. and Zhao, S.J. (2004) The function of chloroplastic NAD(P)H dehydrogenase in tobacco during chilling stress under low irradiance. *Plant Cell Physiol.* 45: 103-108.

Lu, P., Vogel, C., Wang, R., Yao, X. and Marcotte, E.M. (2007) Absolute protein expression profiling estimates the relative contributions of transcriptional and translational regulation. *Nat. Biotechnol.* 25: 117-124.

Murray, D.L. and Kohorn, B.D. (1991) Chloroplasts of *Arabidopsis thaliana* homozygous for the *ch-1* locus lack chlorophyll *b*, lack stable LHCPII and have stacked thylakoids. *Plant Mol. Biol.* 16: 71-79.

Oster, U., Tanaka, R., Tanaka, A. and Rudiger, W. (2000) Cloning and functional expression of the gene encoding the key enzyme for chlorophyll *b* biosynthesis (CAO) from *Arabidopsis thaliana*. *Plant J.* 21: 305-310.

Ozawa, S., Onishi, T. and Takahashi, Y. (2010) Identification and characterization of an assembly intermediate subcomplex of photosystem I in the green alga *Chlamydomonas*

reinhardtii. *J. Biol. Chem.* 285: 20072-20079.

Peng, L., Fukao, Y., Fujiwara, M., Takami, T. and Shikanai, T. (2009) Efficient operation of NAD(P)H dehydrogenase requires supercomplex formation with photosystem I via minor LHCI in Arabidopsis. *Plant Cell* 21: 3623-3640.

Peng, L., Yamamoto, H. and Shikanai, T. (2010) Structure and biogenesis of the chloroplast NAD(P)H dehydrogenase complex. *Biochim. Biophys. Acta* 1807: 945-953

Peng, L. and Shikanai, T. (2011) Supercomplex formation with photosystem I is required for the stabilization of the chloroplast NADH dehydrogenase-like complex in Arabidopsis. *Plant Physiol.* 155: 1629-1639.

Preiss, S. and Thornber, J.P. (1995) Stability of the apoproteins of light-harvesting complex I and II during biogenesis of thylakoids in the chlorophyll *b*-less barley mutant *chlorina f2*. *Plant Physiol.* 107: 709-717.

Salvi, D., Rolland, N., Joyard, J. and Ferro, M. (2008) Purification and proteomic analysis of chloroplasts and their sub-organellar compartments. *Methods Mol. Biol.* 432: 19-36.

Schmid, V.H., Potthast, S., Wiener, M., Bergauer, V., Paulsen, H. and Storf, S. (2002) Pigment binding of photosystem I light-harvesting proteins. *J. Biol. Chem.* 277: 37307-37314.

Schmid, V.H. (2008) Light-harvesting complexes of vascular plants. *Cell. Mol. Life Sci.* 65: 3619-3639.

Schwenkert, S., Umate, P., Dal Bosco, C., Volz, S., Mlcochova, L., Zoryan, M.et al. (2006) PsbI affects the stability, function, and phosphorylation patterns of photosystem II assemblies in tobacco. *J. Biol. Chem.* 281: 34227-34238.

Shevchenko, A., Wilm, M., Vorm, O. and Mann, M. (1996) Mass spectrometric sequencing of proteins silver-stained polyacrylamide gels. *Anal. Chem.* 68: 850-858.

Takabayashi, A., Ishikawa, N., Obayashi, T., Ishida, S., Obokata, J., Endo, T. et al. (2009) Three novel subunits of Arabidopsis chloroplastic NAD(P)H dehydrogenase identified by bioinformatic and reverse genetic approaches. *Plant J.* 57: 207-219.

Tan, S., Cunningham, F.X., Jr. and Gantt, E. (1997a) LhcaR1 of the red alga *Porphyridium cruentum* encodes a polypeptide of the LHCI complex with seven potential chlorophyll *a*-binding residues that are conserved in most LHCs. *Plant Mol. Biol* .33: 157-167.

Tan, S., Ducret, A., Aebersold, R. and Gantt, E. (1997b) Red algal LHC I genes have similarities with both Chl *a*/*b*- and *a*/*c*-binding proteins: A 21 kDa polypeptide encoded by LhcaR2 is one of the six LHC I polypeptides. *Photosynth. Res.* 53: 129-140.

Tanaka, A., Tanaka, Y., Tsuji, H. (1987) Resolution of chlorophyll *a*/*b*-protein complexes by polyacrylamide gel electrophoresis: evidence for the heterogeneity of light-harvesting chlorophyll *a*/*b*-protein complexes. *Plant Cell Physiol*. 28: 1537-1545.

Tanaka, A., Yamamoto, Y. and Tsuji, H. (1991) Formation of chlorophyll-protein complexes during greening 2. Redistribution of chlorophyll among apoproteins. *Plant Cell Physiol*. 32: 195-204.

Tanaka, A. and Melis, A. (1997) Irradiance-dependent changes in the size and composition of the chlorophyll *a-b* light-harvesting complex in the green alga *Dunaliella salina*. *Plant Cell Physiol*.38: 17-24.

Tanaka, A., Ito, H., Tanaka, R., Tanaka, N.K., Yoshida, K. and Okada, K. (1998) Chlorophyll *a* oxygenase (CAO) is involved in chlorophyll *b* formation from chlorophyll *a*. *Proc. Natl Acad. Sci. USA* 95: 12719-12723.

Tanaka, R. and Tanaka, A. (2005) Effects of chlorophyllide *a* oxygenase overexpression on light acclimation in *Arabidopsis thaliana*. *Photosynth. Res.* 85: 327-340.

Terao, T., Yamashita, A. and Katoh, S. (1985) Chlorophyll *b*-deficient mutants of rice II. Antenna chlorophyll *a*/*b*-proteins of photosystem I and II. *Plant Cell Physiol*. 26: 1369-1377.

Tomitani, A., Okada, K., Miyashita, H., Matthijs, H.C.P., Ohno, T. and Tanaka, A. (1999) Chlorophyll *b* and phycobilins in the common ancestor of cyanobacteria and chloroplasts. *Nature* 400: 159-162.

Wang, P., Duan, W., Takabayashi, A., Endo, T., Shikanai, T., Ye, J.Y. et al. (2006) Chloroplastic

NAD(P)H dehydrogenase in tobacco leaves functions in alleviation of oxidative damage caused by temperature stress. *Plant Physiol.* 141: 465-474.

Wientjes, E. and Croce, R. (2011) The light-harvesting complexes of higher-plant Photosystem I: Lhca1/4 and Lhca2/3 form two red-emitting heterodimers. *Biochem. J.* 433: 477-485.

Wittig, I., Braun, H.P. and Schägger, H. (2006) Blue native PAGE. *Nat. Protoc.* 1: 418-428.

Wittig, I. and Schägger, H. (2009) Native electrophoretic techniques to identify protein-protein interactions. *Proteomics* 9: 5214-5223.

Table 1. Chlorophyll contents in wild-type and *ch1-1* plants.

	Wild type	*ch1-1*
Total Chl (nmol / gFW)	1862 ± 125	1090± 137
Chl *a* (nmol / gFW)	1434 ± 96	1090± 137
Chl *b* (nmol / gFW)	428 ± 29	N.D.
Chl *a* / Chl *b*	3.35	N.C.

The chlorophyll levels were determined in 4-week-old wild type and *ch1-1* plants. The data are presented as the mean ± SD of three independent determinations.

Table 2. Chlorophyll fluorescence analysis of wild-type and *ch1-1* plants.

	Fv/Fm	NPQ	qE
wild type	0.794 ± 0.01	1.058 ± 0.142	0.907 ±0.111
ch1-1	0.772 ± 0.01 (97%)	0.72 ± 0.063 (68%)	0.541 ± 0.069 (60%)

The chlorophyll fluorescence was measured in 4-week-old plants (wild type) and 5-week-old plants (*ch1-1*). The data are the mean ± SD of eight independent measurements. The values in parentheses show the relative percentages of *ch1-1* compared with the wild type.

Table 3. List of the detected proteins of PSI and PSII.

	Locus	Symbols	Number of matched peptides (wild type)	Number of matched peptides (*ch1-1)*
PSI core	ATCG00350	PSAA	122	54
complex	ATCG00340	PSAB	122	76
	ATCG01060	PSAC	76	51
	AT4G02770	PSAD-1	122	79
	AT1G03130	PSAD-2	156	76
	AT4G28750	PSAE-1	64	49
	AT2G20260	PSAE-2	41	37
	AT1G31330	PSAF	114	60
	AT1G55670	PSAG	31	23
	AT1G52230	PSAH2	42	25
	AT1G30380	PSAK	21	10
	AT4G12800	PSAL	26	14
	AT2G46820	PSAP	42	33
PSII core	ATCG00020	PSBA	369	361
complex	ATCG00680	PSBB	384	276
	ATCG00280	PSBC	298	275
	ATCG00270	PSBD	142	137
	ATCG00580	PSBE	23	14
	ATCG00710	PSBH	76	117
	ATCG00560	PSBL	10	12
	AT5G66570	PSBO1	227	172
	AT3G50820	PSBO2	190	158
	AT1G06680	PSBP1	152	46
	AT4G21280	PSBQ1	139	101
	AT1G79040	PSBR	26	31
	AT1G44575	PSBS	130	121
	AT3G21055	PSBTN	10	5
	AT4G28660	PSB28	1	1
Light	AT3G54890	LHCA1	37	8
Harvesting	AT3G61470	LHCA2	35	9
Complex I	AT1G61520	LHCA3	173	76

	AT3G47470	LHCA4	66	38
	AT1G45474	LHCA5	21	13
	AT1G19150	LHCA6	5	1
Light Harvesting Complex II	AT1G29910	LHCB1.2	418	90
	AT1G29930	LHCB1.3	30	90
	AT2G34420	LHCB1.5	117	2
	AT2G34430	LHCB1.4	276	2
	AT2G05070	LHCB2.2	263	99
	AT5G54270	LHCB3	49	11
	AT5G01530	LHCB4.1	235	147
	AT3G08940	LHCB4.2	203	69
	AT2G40100	LHCB4.3	32	9
	AT4G10340	LHCB5	258	365
	AT1G15820	LHCB6	186	49

The number of matched peptides was calculated by the total sum of the unique peptides for each protein that was identified in the thylakoid membrane fractions of the wild-type or *ch1-1* plants using the Mascot program.

Table 4. List of the detected proteins of the NDH complex.

	Locus	Symbols	Number of matched peptides (wild type)	Number of matched peptides (*ch1-1*)
Membrane subcomplex	NdhA	ATCG01100	1	0
	NdhE	ATCG01070	7	10
Subcomplex A	NdhH	ATCG01110	5	5
	NdhI	ATCG01090	14	5
	NdhK	ATCG00430	15	9
	NdhM	AT4G37925	9	4
	NdhN	AT5G58260	6	5
	NdhO	AT1G74880	2	6
Subcomplex B	NDF1 (NDH48)	AT1G15980	33	17
	NDF2 (NDH45)	AT1G64770	13	9
	NDF4	AT3G16250	1	2
	NDF6	AT1G18730	1	1
	NDH18	AT5G43750	3	0
	PQL2 (PQL1)	AT3G01440	18	17
Lumen subcomplex	PPL2	AT2G39470	19	11
	CYP20-2	AT5G13120	11	4
	FKBP16-2	AT4G39710	10	11
	PQL1 (PQL2)	AT1G14150	12	8

The number of matched peptides was calculated by the total sum of the unique peptides for each protein that was identified in the thylakoid membrane fractions of the wild-type or *ch1-1* plants using the Mascot program.

Figure legends

Figure 1. Visible phenotypes of *ch1-1*. Wild-type and *ch1-1* plants were grown in soil for 4 weeks at 23°C under constant illumination (70 μmol photons m^{-2} s^{-1}). The *ch1-1* mutant showed retarded growth and pale-green phenotypes.

Figure 2. Immunoblot analyses of the LHC proteins in wild-type and *ch1-1* plants. The total leaf extracts from wild-type and *ch1-1* (corresponding to 2 μg chlorophyll *a*) plants were separated by SDS-PAGE (14% acrylamide gel) for immunoblotting.

Figure 3. Separation and identification of the pigment-protein complexes in wild-type and *ch1-1* plants. The BN-PAGE gels were destained with 20% MeOH and 7% acetic acid to clarify the bands of the pigment-protein complexes. The PSII-LHCII supercomplexes (PSII-SC), the PSII dimer (PSII-D), the PSI-LHCI supercomplex, the PSI monomer (PSI-M), the PSII monomer (PSII-M), the LHCII assembly (CP29-CP24-LHCII trimer), and the LHCII trimer (LHCII-T) were visualized in the BN-gel. The identification of the pigment-protein complexes in wild-type and *ch1-1* plants was based on the 2D-BN/SDS-PAGE that was followed by CBB staining and the immunoblot analysis. The positions of the molecular markers are indicated on the left.

Figure 4. 2D-BN/SDS-PAGE of the thylakoid membranes in wild-type (A) and *ch1-1* (B) plants. The protein identification was performed according to previous reports (Fu et al. 2007; Schwenkert et al. 2006). The positions of the molecular markers are indicated on the left.

Figure 5. Immunoblot analyses of the components of the PSI-LHCI supercomplex (PsaA/PsaB, Lhca1, Lhca2, Lhca3, and Lhca4), the PSII-LHCII supercomplexes (CP43, CP47, Lhcb1, Lhcb2, Lhcb3, Lhcb4, Lhcb5, and Lhcb6), and NDH (NDF1), which was followed by 2D-BN/SDS-PAGE in wild-type (A) and *ch1-1* (B) plants.

Figure 6. The effects of the heat treatment on the trimeric LHCII proteins. An immunoblot analysis with the anti-Lhcb2 antibodies was performed to identify the oligomeric states of the LHCII. The dilution series of the trimeric LHCII following the heat treatments is shown. The asterisk indicates the putative apo-Lhcb2 protein that lacked chlorophyll *a*.

Figure 1

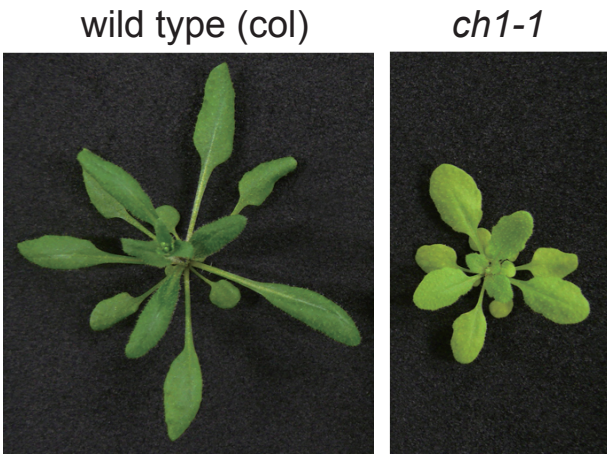

Figure 2

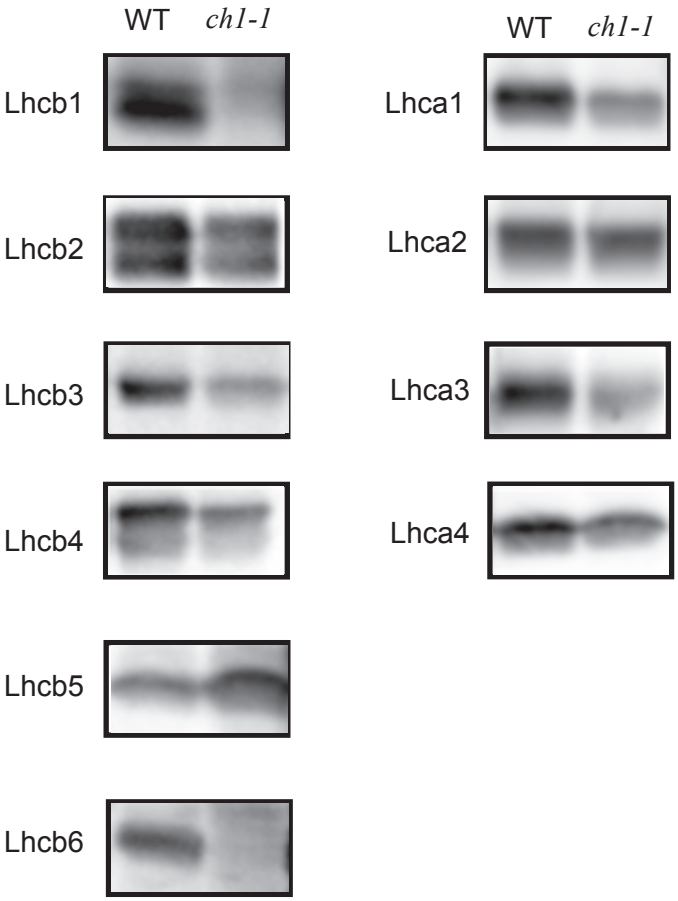
WT
ch1-1
Lhcb1
Lhcb2
Lhcb3
Lhcb4
Lhcb5
Lhcb6
WT
ch1-1
Lhca1
Lhca2
Lhca3
Lhca4

Figure 3

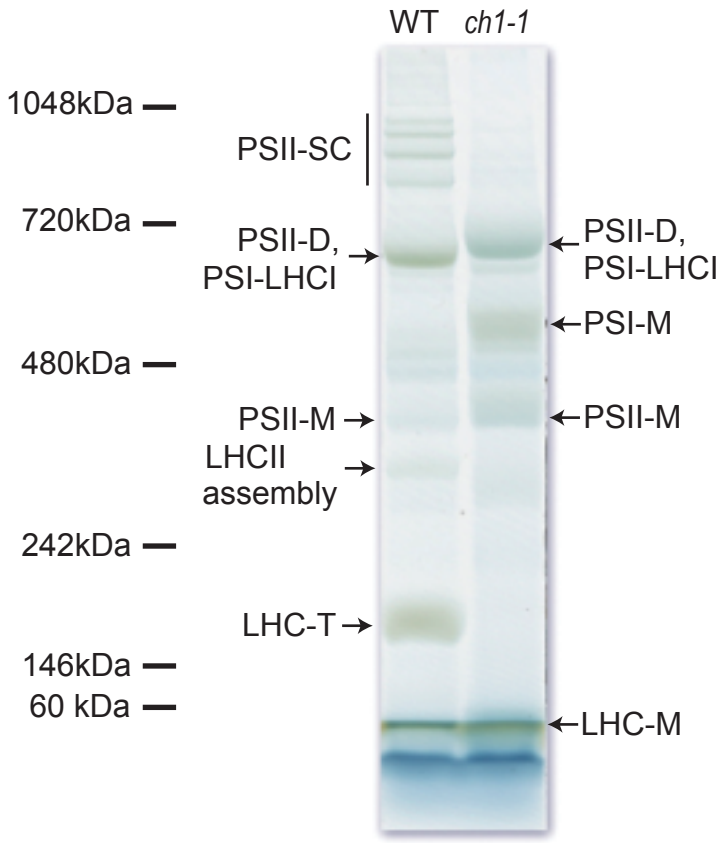
WT
ch1-1
1048kDa
720kDa
480kDa
242kDa
146kDa
60 kDa
PSII-SC
PSII-D,
PSI-LHCI
PSII-M
LHCII
assembly
LHC-T
PSII-D,
PSI-LHCI
PSI-M
PSII-M
LHC-M

Figure 4

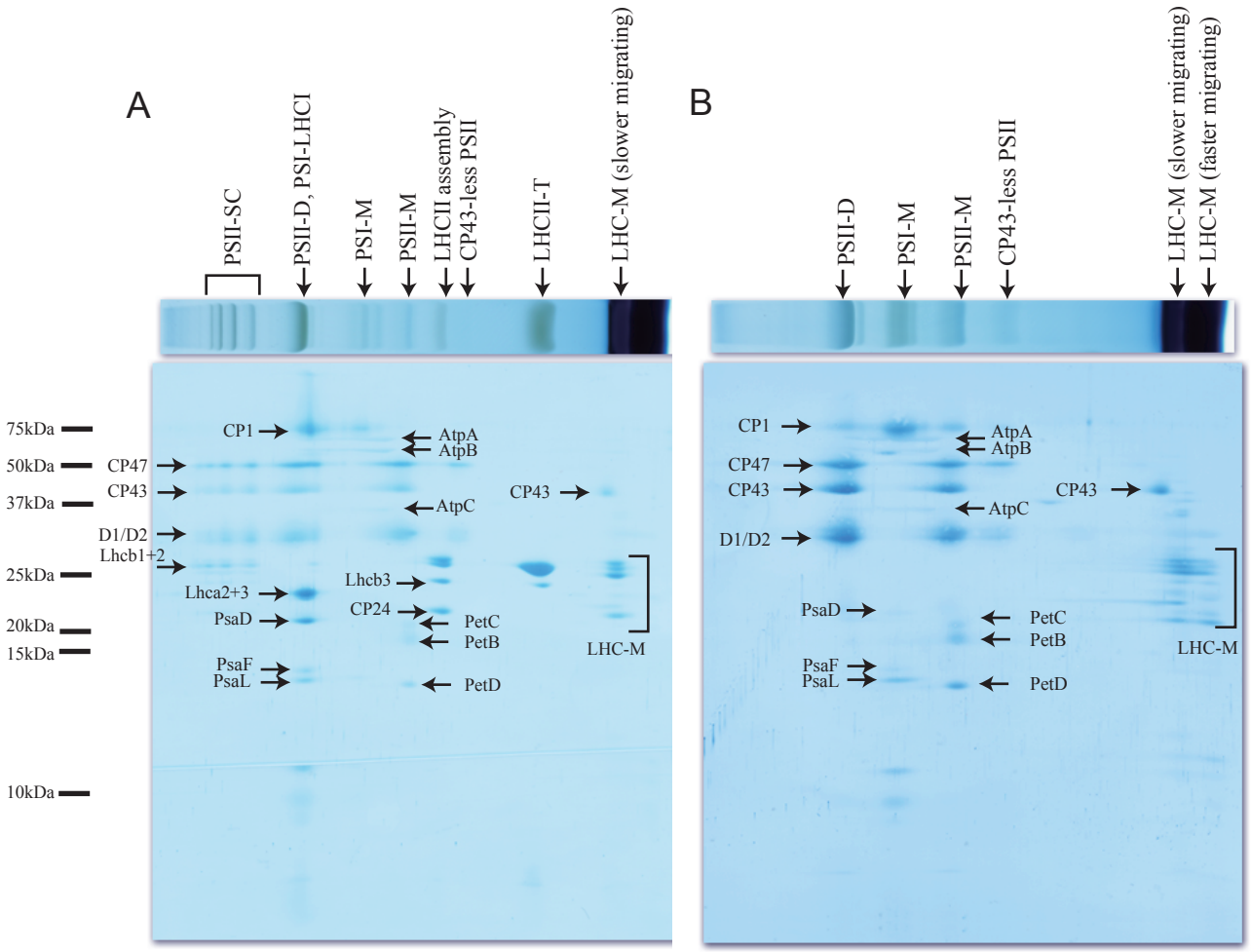
A
PSII-SC
PSII-D, PSI-LHCI
PSI-M
PSII-M
LHCII assembly
CP43-less PSII
LHCII-T
LHC-M (slower migrating)
75kDa
50kDa
37kDa
25kDa
20kDa
15kDa
10kDa
CP1
CP47
CP43
D1/D2
Lhcb1+2
Lhca2+3
PsaD
PsaF
PsaL
AtpA
AtpB
AtpC
Lhcb3
CP24
PetC
PetB
PetD
LHC-M
B
PSII-D
PSI-M
PSII-M
CP43-less PSII
LHC-M (slower migrating)
LHC-M (faster migrating)
CP1
CP47
CP43
D1/D2
PsaD
PsaF
PsaL
AtpA
AtpB
AtpC
PetC
PetB
PetD
LHC-M

Figure 5

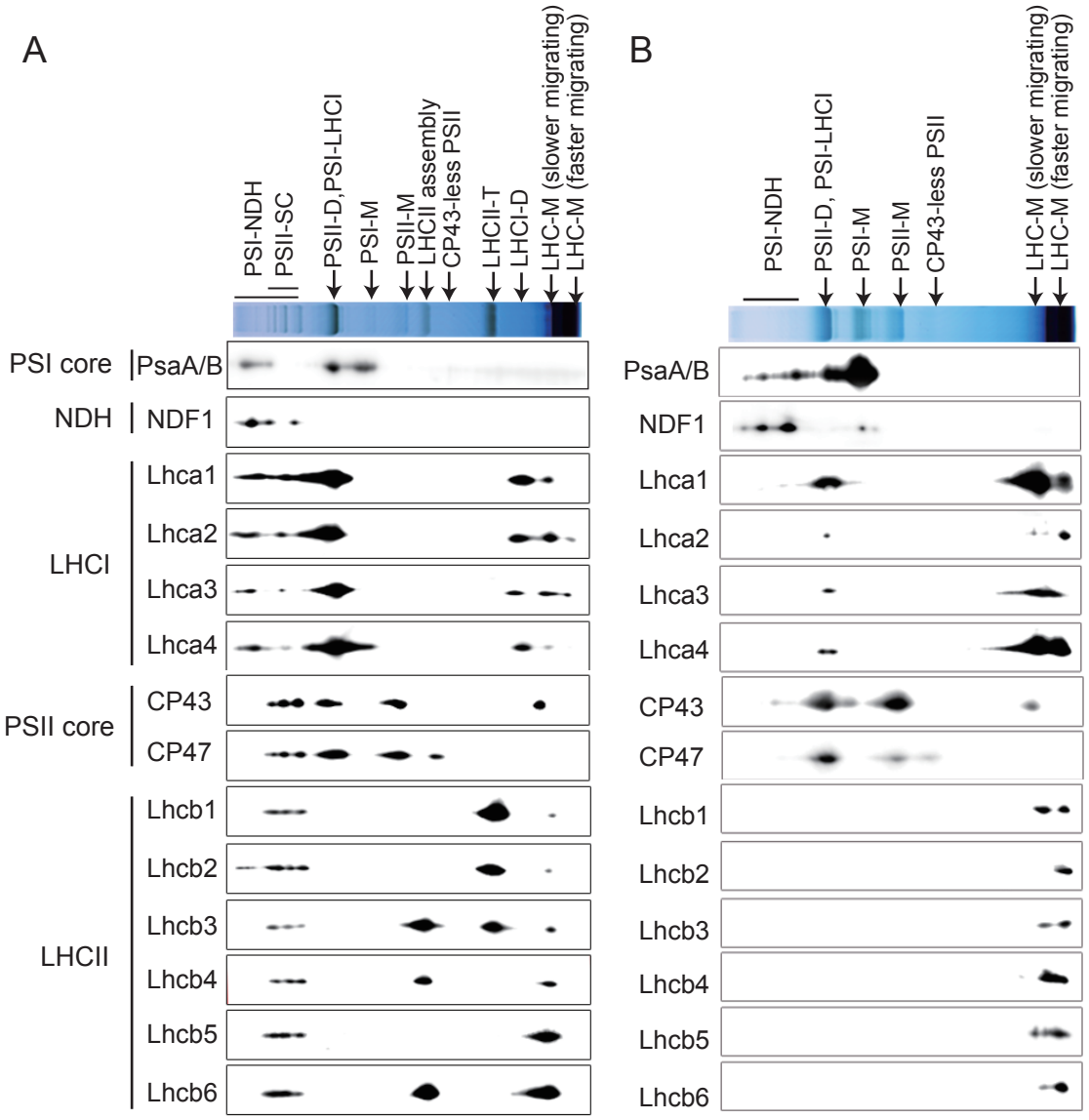
A
PSI-NDH
PSII-SC
PSII-D, PSI-LHCI
PSI-M
PSII-M
LHCII assembly
CP43-less PSII
LHCII-T
LHCI-D
LHC-M (slower migrating)
LHC-M (faster migrating)
PSI core
PsaA/B
NDH
NDF1
LHCI
Lhca1
Lhca2
Lhca3
Lhca4
PSII core
CP43
CP47
LHCII
Lhcb1
Lhcb2
Lhcb3
Lhcb4
Lhcb5
Lhcb6
B
PSI-NDH
PSII-D, PSI-LHCI
PSI-M
PSII-M
CP43-less PSII
LHC-M (slower migrating)
LHC-M (faster migrating)
PsaA/B
NDF1
Lhca1
Lhca2
Lhca3
Lhca4
CP43
CP47
Lhcb1
Lhcb2
Lhcb3
Lhcb4
Lhcb5
Lhcb6

Figure 6

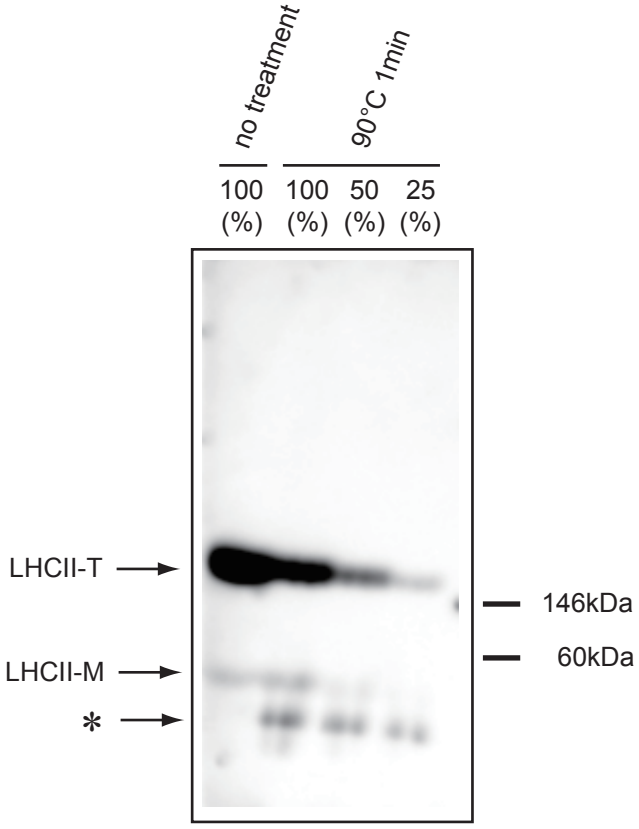
no treatment
90°C 1min
100 (%)
100 (%)
50 (%)
25 (%)
LHCII-T
LHCII-M
*
146kDa
60kDa